J. Synchrotron Rad. (1998). **5**, 774–776

Design of an 18 m spherical-grating monochromator at UVSOR

Hiroaki Yoshida*† and Koichiro Mitsuke

Department of Vacuum UV Photoscience, Institute for Molecular Science, Myodaiji, Okazaki 444, Japan. E-mail: hyoshida@sci.hiroshima-u.ac.jp

(*Received 4 August 1997; accepted 18 November 1997*)

An 18 m spherical-grating monochromator with high resolution and high photon flux has been developed at the bending-magnet beamline BL2B2 of the UVSOR facility in the Institute for Molecular Science. The monochromator is designed to cover the energy range 20–200 eV by using three gratings: G1 (2400 lines mm^{-1}, R = 18 m) at 80–200 eV; G2 (1200 lines mm^{-1}, R = 18 m) at 40–100 eV; G3 (2400 lines mm^{-1}, R = 9.25 m) at 20–50 eV. A resolving power of 5000 and a photon flux of more than 10^{10} photons s^{-1} are expected at a 100 mA ring current. A small including angle of 140° is adopted for G3 and two plane mirrors coated with aluminium are located between G3 and the exit slit as optical filters. These geometrical devices may contribute significantly to the reduction of the high-order lights.

Keywords: spherical-grating monochromators; vacuum UV; high resolution; ray tracing.

1. Introduction

A new monochromator has been designed at beamline BL2B2 of UVSOR to study ionization satellites and multiply excited neutral states of molecules, which often exist in the energy range 20–200 eV (Yoshida & Mitsuke, 1996). A spherical-grating monochromator (SGM) was chosen to satisfy both high resolution and high photon flux (Chen & Sette, 1989; Yagishita *et al.*, 1991; Masui *et al.*, 1992). An SGM with a large radius of curvature is well known to have a resolving power of more than 10 000 (Shigemasa *et al.*, 1995). However, it is difficult to achieve such a high resolving power at the bending-magnet beamline of UVSOR because of the relatively large vertical size of an electron beam (σ_v = 0.27 mm) and a moderate emittance (ε_v = 1.15 × $10^{-8}\pi$ m rad). It is, therefore, planned to realize both a resolving power of 5000 and a photon flux of the order of 10^{10} photons s^{-1} at a 100 mA ring current. In this report, the optical design of the beamline and monochromator are presented.

2. Optical design

2.1. *Layout*

A schematic layout of the beamline is shown in Fig. 1. The optical system consists of two prefocusing mirrors (M0 and M1), a fixed entrance slit (*S*1), an aperture (AP), a spherical grating (G1, G2 or G3), two folding mirrors (M2 and M3), a movable exit slit (S2) and a refocusing mirror (M4).

† Present address: Department of Material Science, Hiroshima University, Kagamiyama, Higashi-Hiroshima 739, Japan.

Table 1
Mirror parameters of the 18 m SGM.

	M0	M1	M2	M3	M4
Shape	Elliptical†	Spherical	Plane	Plane	Toroidal
Radii‡ $R \times \rho$ (mm)¶	28914§	23405			18341 × 202.2
Material	Quartz	Quartz	Quartz	Quartz	Quartz
Coating (nm)	Au 100	Au 100	Al 100	Al 100	Au 100
Reflective area $L \times W$ (mm)	500 × 20	400 × 34	250 × 24	600 × 24	300 × 50
Microroughness†† (Å r.m.s.)		3.29	3.08	1.42	5.0
Grazing angle (°)	6.5	5.0	15.0	5.0	5.0

† Elliptically bent plane mirror by way of Hiraya *et al.* (1992). ‡ Measured using a Newton gauge. § Radius at the centre of the mirror. ¶ Tangential (R) × sagittal (ρ). †† Measured by using a Zygo heterodyne profiler-5500.

The first mirror, M0, which is located 2.136 m downstream from the source point in the electron storage ring, deflects the photon beam by 13°. Vertical and horizontal acceptance angles of this mirror are 6 and 15 mrad, respectively. It serves as a horizontal focusing mirror with a focal distance of 7 m. This mirror is installed in the same vacuum chamber as a prefocusing mirror of the neighbouring beamline BL2B1. Spatial restriction imposed by beamline BL2B1 determines the axis of our monochromator. The vertical prefocusing mirror, M1, is placed 1.8 m behind M0 with a demagnification of 3:1 and a grazing angle of 5°. To decrease distortion induced by heat load, M0 and M1 are equipped with water-cooling systems.

The monochromator is designed to cover the energy range 20–200 eV with three gratings: G1 (2400 lines mm^{-1}, R = 18 m) at 80–200 eV; G2 (1200 lines mm^{-1}, R = 18 m) at 40–100 eV; G3 (2400 lines mm^{-1}, R = 9.25 m) at 20–50 eV. The including angles are 160° for G1 and G2 and 140° for G3. The directions of the incident and exit photon beams are fixed. The arm length of S1 from the grating is fixed at 2 m, while that of S2 varies from 4.18 to 4.58 m. A wavelength-scanning mechanism is very simple because movement of the grating is confined only to mechanical rotation. A set of optical filters, *i.e.* plane mirrors M2 and M3, are inserted across the photon beam between G3 and S2, which may significantly reduce the high-order lights of G3. These mirrors can be removed from the optical path without breaking vacuum when G1 or G2 is chosen. The coma aberration of spherical gratings is expected to be greatly decreased by the aperture placed 1 m from S1.

The refocusing mirror, M4, is located 1.46 m downstream from the mean position of S2, deflecting the photon beam by 10° to make it horizontal. Demagnifications in the vertical and horizontal directions are 1:1 and 2.75:1, respectively. The distance from the source point to the sample point is about 14.7 m.

Parameters of the optical elements are summarized in Tables 1 and 2 (Yoshida & Mitsuke, 1997). Mirror M0 is fabricated by Hidaka Kougaku Kenkyusyo Inc. (Japan) and the other mirrors by Optron Inc. (Japan). All the optical elements are made of quartz coated with Au, except M2 and M3 which are coated with Al to prevent substantially the reflection of the high-order lights. Ion-etched holographic laminar gratings are manufactured by Jobin-Yvon, Div. of Instruments S. A. (France). Slope errors of G1, G2 and G3 are 0.28, 0.25 and 0.18 arcsec, respectively.

2.2. *Resolution*

The estimation of the resolution of a grating monochromator has been fully discussed in the literature (Howells, 1986; Shige-

Table 2
Grating parameters of the 18 m SGM.

	G1	G2	G3
Shape	Spherical	Spherical	Spherical
Radius (mm)†	17987 ± 18	17987 ± 18	9246 ± 6
Groove density (lines mm^{-1})	2400	1200	2400
Duty ratio‡§	0.61	0.675	0.62
Groove depth (nm)§	11.4	22.6	23.5
Au coating (nm)	40 ± 4	40 ± 4	40 ± 4
Material	Quartz	Quartz	Quartz
Ruled area $L \times W$ (mm)	130 × 20	130 × 20	130 × 20
Size $L \times W \times T$ (mm)	140 × 30 × 25	140 × 30 × 25	140 × 30 × 25
Microroughness (Å r.m.s.)¶	3.6	<5	<5
Slope error (arcsec)††	<0.28	0.25	0.18
Including angle (°)	160	160	140

† Measured by Foucault knife-edge test with an optical bench. ‡ Groove width/pitch. § Measured by using scanning tunnelling microscope Nanoscope II. ¶ Measured by using interferential microscope Zygo 2D. †† Measured by using a long-trace profiler.

masa *et al.*, 1995). The total bandwidth, $\Delta\lambda$, is expressed by the root mean square of terms for the contributions due to the entrance slit width ($\Delta S1$), the exit slit width ($\Delta S2$), the aberration (ΔY_{ab}) of the grating, the slope error (σ_{sl}) of the grating, and the diffraction limit:

$$\Delta\lambda = [\Delta\lambda_{S1}^2 + \Delta\lambda_{S2}^2 + \Delta\lambda_{ab}^2 + \Delta\lambda_{sl}^2 + \Delta\lambda_{limit}^2]^{1/2}, \quad (1)$$

$$\Delta\lambda_{S1} = \Delta S1\, d\cos\alpha/r_1, \quad (2)$$

$$\Delta\lambda_{S2} = \Delta S2\, d\cos\beta/r_2, \quad (3)$$

$$\Delta\lambda_{ab} = \Delta Y_{ab}\, d\cos\beta/r_2, \quad (4)$$

$$\Delta\lambda_{sl} = 2d\sigma_{s1}(\cos\alpha + \cos\beta), \quad (5)$$

$$\Delta\lambda_{limit} = \lambda/N. \quad (6)$$

Here, d is the groove width of the grating, N is the number of participating grooves, r_1 and r_2 are the entrance and exit focal lengths, respectively, and α and β are the incident and diffraction angles, respectively. The term due to the diffraction limit is so small that it is ignored. Among several possible origins of ΔY_{ab}, the coma aberration is considered to reduce most seriously a resolving power. Indeed, the total resolution is negligibly affected by other terms such as spherical aberration, astigmatism and astigmatic coma. Substituting a well known expression of the coma aberration of a spherical grating for (4), we obtain (7),

$$\Delta\lambda_{coma} = 3dw^2(T_1/r_1 \sin\alpha + T_2/r_2 \sin\beta)/2, \quad (7)$$

$$T_1 = \cos^2\alpha/r_1 - \cos\alpha/R, \quad (8)$$

$$T_2 = \cos^2\beta/r_2 - \cos\beta/R, \quad (9)$$

where R is the radius of the grating and w is the half-length of the illuminated area of the grating.

Fig. 2 shows the calculated resolving powers at the entrance and exit slit widths of 50 µm. The total resolving power higher than 5000 can be realized at 100–150 eV by using G1 and at 20–70 eV by using either G2 or G3. The slope error term, $\Delta\lambda_{sl}$, is not so important because of the small σ_{sl} value for a spherical surface. For each grating the total resolving power is dominated mainly by the entrance slit width in the higher energy side and by the coma aberration in the lower energy side. To achieve a resolving power of 5000, we must reduce the entrance slit width to 25 µm in the higher energy side for G1 and G2 and decrease the coma aberration by shutting off a diverged light by reducing the aperture width to 3.7 mm.

2.3. *Photon fluxes of the first- and second-order lights*

Throughput of the present 18 m SGM beamline is expressed as

$$\varepsilon = \varepsilon_{acc}\varepsilon_{diff}R_G R_0 R_1 R_2 R_3 R_4. \quad (10)$$

Here, R_G, R_0, R_1, R_2, R_3 and R_4 are the reflectivities of the grating, M0, M1, M2, M3 and M4, respectively; ε_{acc} is the accepting efficiency of the beamline, which includes those of both the slit and the aperture; ε_{diff} is the diffraction efficiency of the grating calculated by scalar theory formulae (Shigemasa *et al.*,

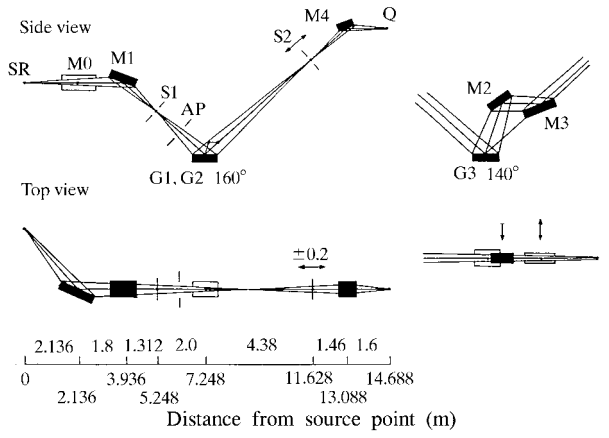

Figure 1
Schematic layout of renewed BL2B2 equipped with an 18 m SGM. Two optical paths with including angles of 160° for G1 and G2 and 140° for G3 are indicated. SR: synchrotron radiation source point; M0: elliptically bent plane mirror; M1: spherical mirror; S1: entrance slit; AP: aperture; G1, G2 and G3: spherical gratings; M2 and M3: plane mirrors; S2: exit slit; M4: toroidal mirror; Q: sample point.

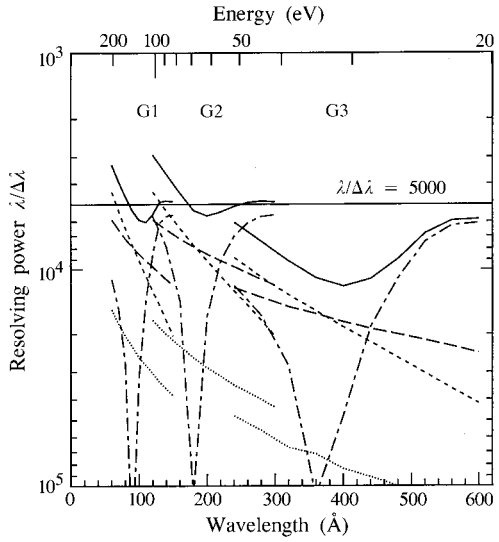

Figure 2
Calculated resolving powers of the present 18 m SGM at the entrance and exit slit widths of 50 µm: total resolving power (——) and resolving powers by the entrance slit width (- - -), the exit slit width (– – –), the coma aberration (– - –) and the slope error (···). The horizontal line indicates a resolving power of 5000.

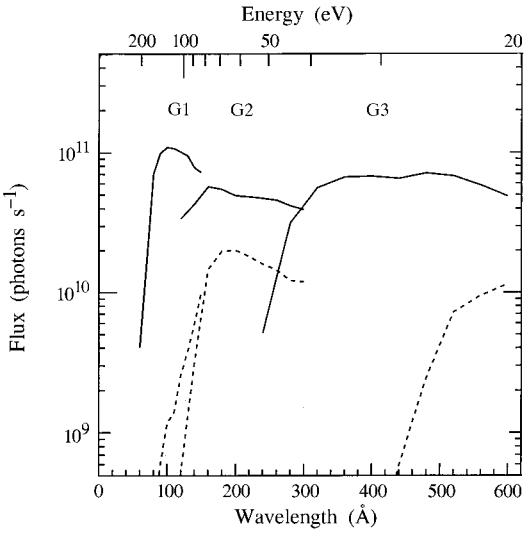

Figure 3
Calculated throughput photon fluxes of the present 18 m SGM beamline for 100 mA ring current with a resolving power of 5000: first-order light (—), second-order light (- -).

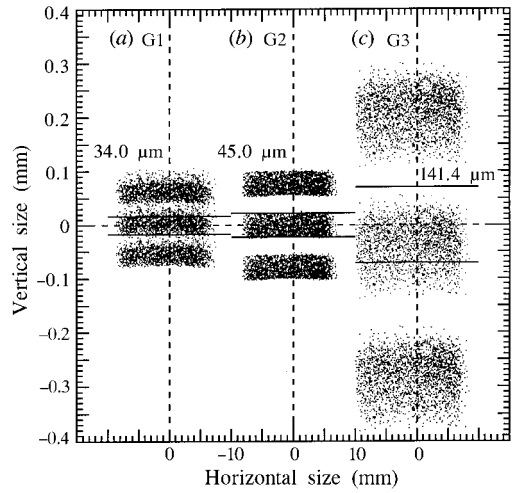

Figure 4
Image patterns at the exit slit obtained by ray tracing with photon wavelengths of (*a*) 60 and 60 ± 0.012 Å for G1, (*b*) 180 and 180 ± 0.036 Å for G2, and (*c*) 600 and 600 ± 0.12 Å for G3. Pairs of horizontal lines indicate the widths of the exit slit corresponding to a resolving power of 5000.

1995). The calculated throughput spectra of the first-order light at a fixed resolving power of 5000 are shown in Fig. 3. The throughput photon flux is more than 1×10^{10} photons s^{-1} for a 100 mA ring current in a wide wavelength region of 65–600 Å by interchanging the three gratings.

The calculated throughput spectra of the second-order light are also indicated in Fig. 3. The reflectivities of M0, M1 and M4 are quite smaller at $\lambda < 60$ Å than at $150 > \lambda > 60$ Å. The ratio between the fluxes of the second- and the first-order lights from G1 is, thus, less than 0.1. The reflectivities of M0, M1 and M4 are almost constant at $300 > \lambda > 80$ Å so that the above flux ratio increases to 0.4 when G2 is utilized. In the case of G3, the reflectivities of M2 and M3 coated with Al are practically disregarded for the second-order light. Therefore, the flux ratio is quite small except in a wavelength region above 500 Å.

2.4. *Ray tracing*

Fig. 4 shows image patterns at the exit slit obtained by ray tracing with photon wavelengths of (*a*) 60 and 60 ± 0.012 Å for G1, (*b*) 180 and 180 ± 0.036 Å for G2, and (*c*) 600 and 600 ± 0.12 Å for G3. The beam emittance parameters of the light source assumed in the ray tracing are $\sigma_H = 0.41$ mm, $\sigma_V = 0.29$ mm, $\sigma'_H = 0.39$ mrad and $\sigma'_V = 0.06$ mrad. The exit slit is placed at the focal distances for the respective gratings. The widths of the exit slit corresponding to an expected resolving power of 5000 are also indicated by pairs of horizontal lines. In every case, the central wavelength is well resolved from two neighbouring wavelengths. Hence, it is concluded that the present monochromator will provide a resolving power of 5000. Image patterns at the sample point obtained by ray tracing at the entrance and exit slit widths of 50 μm are less than 2 mm in diameter.

3. Summary

An 18 m spherical-grating monochromator is designed to cover the energy range 20–200 eV with the three gratings. The two folding mirrors between G3 and S2 effectively decrease higher-order contributions in the energy range 25–50 eV. It is concluded that, by adjusting the widths of S1 and AP, throughput photon flux of more than 10^{10} photons s^{-1} for 100 mA ring current will be obtained at 20–190 eV with a resolving power of 5000. Ray-tracing results at S2 also support the conclusion.

This monochromator was manufactured by Toyama Co., Ltd (Japan) and assembled at UVSOR in May 1997. At present, the optical alignment is being performed.

The authors would like to acknowledge gratefully useful suggestions from Professor Atsunari Hiraya of Hiroshima University, Professor Akira Yagishita of the Photon Factory, Dr Yonglian Yan of BSRL in China, and Professor Eiji Ishiguro of Ryukyu University.

References

Chen, C. T. & Sette, F. (1989). *Rev. Sci. Instrum.* **60**, 1616–1621.
Hiraya, A., Horigome, T., Okada, N., Mizutani, N., Sakai, K., Matsudo, O., Hasumoto, M., Fukui, K. & Watanabe, M. (1992). *Rev. Sci. Instrum.* **63**, 1264–1268.
Howells, M. R. (1986). *Gratings and Monochromators*, in *X-ray Data Booklet*. Center for X-ray Optics, Lawrence Berkeley Laboratory, Berkeley, CA 94720, USA.
Masui, S., Shigemasa, E. & Yagishita, A. (1992). *Rev. Sci. Instrum.* **63**, 1330–1333.
Shigemasa, E., Yan, Y. & Yagishita, A. (1995). KEK Report 95–2. KEK, Tsukuba, Japan.
Yagishita, A., Hayaishi, T., Kikuchi, T. & Shigemasa, E. (1991). *Nucl. Instrum. Methods*, A**306**, 578–583.
Yoshida, H. & Mitsuke, K. (1996). *UVSOR Activity Report 1995*, pp. 112–113. UVSOR, Institute for Molecular Science, Okazaki 444, Japan.
Yoshida, H. & Mitsuke, K. (1997). *UVSOR Activity Report 1996*, pp. 114–115. UVSOR, Institute for Molecular Science, Okazaki 444, Japan.